Elsevier Editorial System(tm) for Carbohydrate Polymers
Manuscript Draft

Manuscript Number: CARBPOL-D-19-01942R2

Title: Fabrication and characterization of a novel konjac glucomannan-based air filtration aerogels strengthened by wheat straw and okara

Article Type: Research Paper

Keywords: Konjac glucomannan; Air filtration aerogel; Wheat straw; Okara; Mechanical property; Hydrophobic property

Corresponding Author: Professor Fatang Jiang, PhD

Corresponding Author's Institution: Hubei University of Technology

First Author: Weiling Wang

Order of Authors: Weiling Wang; Ying Fang; Xuewen Ni, PhD; Kao Wu, PhD; Yixin Wang; Saffa B. Riffat, PhD; Fatang Jiang, PhD

Abstract: The konjac glucomannan (KGM)-based aerogel as an air filtration material was fabricated through sol-gel and freeze-drying methods. Results showed that gelatin and starch addition could increase the filtration efficiency and compressive strength of aerogel significantly, due to the appearance of more microporous structure and the formation of dense structure in aerogel. The addition of wheat straw could decrease the filtration resistance and increase the breathability of KGM-based aerogel, which was attributed to the multi-cavities of wheat straw. The aerogel with wheat straw had a filtration efficiency of 93.54% for particle matters ≥ 0.3 μm, a filtration resistance 29 Pa, and an air permeability 271.42 L/s·m2. Okara addition could increase the hydrophobicity of KGM-based aerogel by increasing the water contact angle and decreasing the equilibrium water content. The water contact angle of the aerogel containing okara reached 105.4°, and the equilibrium water content was decreased by 17.03%-81.10% compared with that without okara, with relative humidity 0%-80%. The results demonstrated that the KGM-based aerogel had good performance on filtration, mechanical and hydrophobic properties, indicating high potential application as an air filtration material.

***Highlights (for review)**

1. KGM-based aerogel with good filtration and hydrophobic properties was prepared.

2. Starch and gelatin addition enhanced mechanical and filtration property of aerogels.

3. Wheat straw addition improved filtration resistance and gas permeability of aerogels.

4. Okara addition could improve aerogel hydrophobicity.

Fabrication and characterization of a novel konjac glucomannan-based air filtration aerogels strengthened by wheat straw and okara

Weiling Wang[a], Ying Fang[a], Xuewen Ni[a], Kao Wu[a], Yixin Wang[b], Fatang Jiang[a,b,*], Saffa B. Riffat[b,**]

[a] School of Bioengineering and Food Science, Hubei University of Technology, Wuhan 430068, China

[b] University of Nottingham, NG7 2RD, UK

* Corresponding author at: School of Bioengineering and Food Science, Hubei University of Technology, Wuhan 430068, China.

** Corresponding author at: University of Nottingham, NG7 2RD, UK.

E-mail addresses: JIANGFT@mail.hbut.edu.cn (F. Jiang), saffa.riffat@nottingham.ac.uk (Saffa. R).

ABSTRACT

The konjac glucomannan (KGM)-based aerogel as an air filtration material was fabricated through sol-gel and freeze-drying methods. Results showed that gelatin and starch addition could increase the filtration efficiency and compressive strength of aerogel significantly, due to the appearance of more microporous structure and the formation of dense structure in aerogel. The addition of wheat straw could decrease the filtration resistance and increase the breathability of KGM-based aerogel, which was attributed to the multi-cavities of wheat straw. The aerogel with wheat straw had a filtration efficiency of 93.54% for particle matters ≥ 0.3 μm, a filtration resistance 29 Pa, and an air permeability 271.42 L/s·m^2. Okara addition could increase the hydrophobicity of KGM-based aerogel by increasing the water contact angle and decreasing the equilibrium water content. The water contact angle of the aerogel containing okara reached 105.4°, and the equilibrium water content was decreased by 17.03%-81.10% compared with that without okara, with relative humidity 0%-80%. The results demonstrated that the KGM-based aerogel had good performance on filtration, mechanical and hydrophobic properties, indicating high potential application as an air filtration material.

Keywords: Konjac glucomannan; Air filtration aerogel; Wheat straw; Okara; Mechanical property; Hydrophobic property

1. Introduction

In recent decades, the fast economic growth of modern society has accompanied with serious environmental air pollution, threatening humans' health and life (Chow, & Judith, 2006). As the main cause of air pollution, harmful particles in the air come from many aspects and are mainly divided into three categories according to their types: physical pollution (particulate matter, dust, pollen, etc.), chemical pollution (SOX, nitrogen oxides and volatile organic compounds, etc.) and biological contamination (bacteria, mold spores, viruses, etc.) (Landrigan, 2017; Pope, et al., 2002; Anderson, Thundiyil, & Stolbach, 2012). PM2.5 (particle sizes < 2.5μm) is the main cause of air pollution (Brunekreef, & Hoffmann, 2016), and could seriously threaten people's health (Cohen, et al., 2005; B.R. Gurjar, et al., 2010; Russell, & Brunekreef, 2009).

Air filtration is the most effective way to solve air pollution problems (Sutherland, 2008). Various filter materials have been used for air filtration, such as fiber filter materials, composite filter materials, and functional filter materials (Antonicelli, Bilò, Pucci, Schou, & Bonifazi, 1991). Fiberglass and quartz fiber are used for air filtration with 95% filtration efficiency (Akbarnezhad, Amini, Goharrizi, Rainey, & Morawska, 2017). Nano-TiO_2 photocatalytic materials have shown attractive application prospects in air purification, and it can absorb harmful gases in air (CO, SO_2, NH_3, NO_x, and VOC), achieving the purpose of sterilization and air filtration without secondary pollution (Suarez, et al., 2011). Activated carbon fibers, nanofibers, and photocatalytic materials are often used as air filtration materials in air conditioning systems (HVAC) (Tang, et al., 2018; Park, Yoon, & Hwang, 2011; Pigeot-Remy, et al., 2014). These air filter materials not only have a limited source of raw materials but are also not environmentally friendly. Therefore, there is an urgent need to develop new environmentally friendly air filter materials.

As classical porous materials, aerogels are considered to be good air filtration materials due to their continuous three-dimensional network structure, adjustable density, high specific surface area, and high porosity (Kim, Chase, & Jana, 2015). Plant polysaccharide aerogels, such as cellulose aerogels (Shi, Lu, Guo, Liu, & Cao, 2015; Xu, Bao, Xu, Wang, & Sun, 2015), starch aerogels (García-González, Uy, Alnaief, & Smirnova, 2012) and sodium alginate aerogels (Wang, et al., 2016), not only have the physical properties of aerogel, but also their raw materials have abundant resources, good biosafety, and environmentally friendly advantages. However, the problems of poor mechanical and hydrophobic properties limit the application of plant polysaccharide aerogels for air filtration purposes (Zhu, Hu, Jiang, Liu, & Li, 2018). Konjac glucomannan (KGM) is a high molecular weight water-soluble polysaccharide (Fang, & Wu, 2004; Davé, & McCarthy, et al., 1997), and it was suitable for aerogel preparation with high specific surface area (as high as 51.8 m^2/g) (Jiang, 2013; Wang et al., 2017). Gelatin is rich in hydroxyl, carboxyl and amino groups in its molecular chain, making it easy to gel and functionalize, and so it can be the starting material for constructing a 3D structure (Wang, et al., 2016). Porous gelatin networks for tissue engineering, flame retardancy, oil/water separation, and contaminant adsorption have been developed (Kang, Tabata, & Ikada, 1999; Huang, et al., 2017; Li, et al., 2016), and incorporating biobased gelatin to poly (vinyl alcohol) / clay aerogels could improve aerogel strength and flame retardancy (Wang, et al., 2017). Starch has a special retrogradation phenomenon that the starch molecules will rearrange into ordered crystals when fully gelatinized starch is cooled at a lower temperature or slowly dehydrated and dried (Jiamjariyatam, Kongpensook, & Pradipasena, 2014). As a by-product of wheat, wheat straw is usually incinerated and causes environmental pollution, however, it can be also used to produce air filtration materials (Wang et al., 2017). Okara is a by-product of soy milk or tofu and contains a large amount of insoluble dietary fiber residue (Mateos-Aparicio, Redondo-Cuenca, Villanueva-Suárez, Zapata-Revilla, & Tenorio-Sanz, 2010). In the okara, the dietary fiber content reaches 50% to 70%, fat content is 8% to 11%, and protein content is 19% to 23% (Redondo-Cuenca, Villanueva-Suárez, & Mateos-Aparicio, 2008). Appropriate addition of different polymers to the composite material could improve functional properties (Corobea et al., 2016), and therefore aerogels with air filtration function may be produced with these environmentally friendly materials (KGM, gelatin, starch, wheat straw, okara). The study aimed to investigate the pore structure, mechanical and filtration properties (DEHS (dioctyl sebacate) as an aerosol for filtration property) of KGM/gelatin/starch aerogels, and the filtration and hydrophobic properties of KGM/gelatin/starch-based aerogels strengthened by wheat straw and okara. This study can contribute to the research and application of KGM-based aerogels as air filtration material.

2. Materials and method

2.1. Materials

Konjac glucomannan (KGM) was supplied by Licheng Biological Technology Co., Ltd. (Wuhan, China). Potato starch (S) was obtained from Wuhan Lin He Ji Food Co., Ltd. (Wuhan, China). Gelatin (G) was purchased from Sinopharm Chemical Reagent Co., Ltd (Shanghai, China). Raw wheat straw (WS) and okara (O) were obtained from farmhouses in Wuhan. Both the raw wheat straw and okara were ground into flours by a grain pulverizer and screened through a 160 mesh sieve before use.

2.2. KGM-based aerogel preparation

The preparation of KGM-based aerogel was based on the previous research (Wang, 2018) with minor modification as illustrated in Fig. 1. Gelatin, starch, wheat straw, okara, KGM were dissolved in double-distilled water (90 ℃) in order and stirred at a speed of 1000 rpm for 1 h to mix the entire solution. And then the sol was injected into two different sizes of cylindrical mold (diameter 34.8 mm and height 18 mm, diameter 142 mm and height 10 mm) and placed in a 4 ℃ refrigerator for aging for 2 h, after that, it would be placed in a -25 ℃ ultra-low temperature refrigerator for 8 h. The frozen samples were pot in a vacuum freeze dryer (Modulyod-230, Thermo Electron Corporation, USA) (-55 °C, 1 Pa) for 24 h to be completely freeze-dried. Aerogel samples were coded as the form of K0G0S0WS(O)0, and the number after the letter indicates the mass percentage of the component. All aerogel samples were stored in a drying vessel (50 ℃) for 12 h before use.

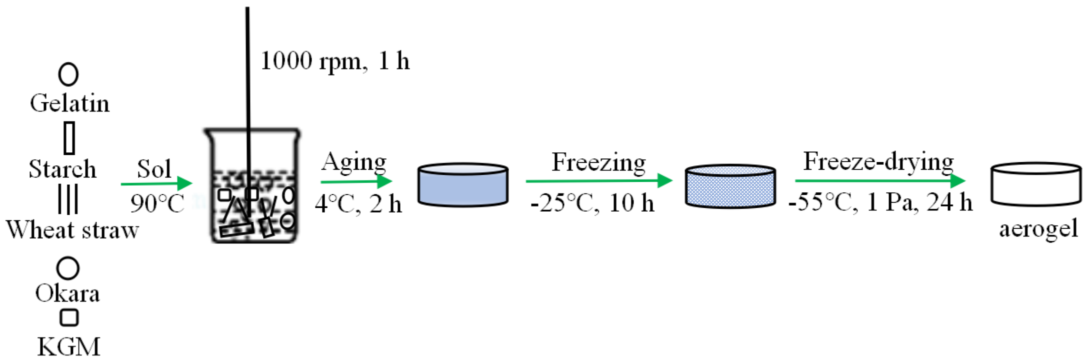

Fig. 1. Schematic procedure of preparing KGM-based aerogels.

2.3. Characterization

2.3.1. Filtration performance test

The filtration efficiency, filtration resistance and breathability of samples were tested using a LZC-K1 type filter comprehensive performance test bench (LZC-K1, Suzhou Huada, China). The test bench mainly included test channels (including filter fixtures), flow control units, atomized aerosol generators, particle counters, pressure gauges, fans, and other components, as well as control units and data acquisition software. The effective test area was 15 cm ×15 cm, and the filtration efficiency and filtration resistance were tested by feeding an electrically neutral monodisperse DEHS aerosol to samples at a median diameter of 0.3-10 μm. The filter piezoresistive force was coordinated by the flowmeter and two electronic pressure sensors. The breathability test was performed by measuring the air flow rate through the sample per unit area under a pressure of 200 Pa and converted it into the air permeability. All filtration tests were performed at 24 ± 2 ℃, the flow rate of filtration was 32 L/min for resistance and filtration efficiency tests, and the time for each filtration test was 1 min.

2.3.2. Microstructure and pore size distribution

Prior to test, aerogel samples were cut into small pieces (5 mm × 5 mm × 1 mm). The samples were fixed on a stainless steel sample stage with conductive paste before sputtered with gold for 80 s (JFC 1600, JEOL Ltd, Japan). Then the surface microstructure was observed by a scanning electron microscopy (SEM) (JSM6390LV, JEOL, Japan) at magnifications of ×50, ×100, ×500, ×850, ×1000. The pore size distribution was evaluated by Image Pro Plus software (Media Cybernetics Inc, Maryland, America), and for each aerogel sample, six representative SEM images were used.

2.3.3. Mechanical property

The mechanical property test of aerogel samples was determined by a Texture analyzer (TA. XT Plus, Stable Micro Systems, Surrey, UK) equipped with a flat bottom probe (No. 10585), based on the method in previous research (Wang, 2018) with minor modification. Double compression mode was adopted with compression percentage 30% and compression rate 1.00 mm/s, and the trigger force was 1.00 N. The parameter of hardness was determined, which was the maximum force (F) during the first cycle of compression. S represents the initial area (mm^2) of samples in contact with the probe, so the sress (σ) was calculated by the following standard equation (Eq. (1)):

$$\sigma = \frac{F}{S} \quad (1)$$

2.3.4. FTIR analysis

Attenuated total reflection was collect at 25 ℃ by using a fourier transform infrared spectroscopy (FTIR) spectrometer (VERTEX 70, Bruker Co., Ltd Germany) equipped with a horizontal attenuated total reflectance (ATR) in the range of 4000-650 cm^{-1}. Data were collected in 32 scans at a resolution of 4 cm^{-1}.

2.3.5. Water contact angle

The water contact angle measurements of aerogel samples were tested at 25 ℃ by a contact angle analyzer (DSA25, Krüss Co., Ltd, Germany) equipped with a charge coupled device (CCD) camera and an image analysis software. The contact angle was measured after the water droplets (5.0 μL) were deposited on the aerogel samples surface (2.0 cm × 1.0 cm) for 10s (Jin, Han, Li, & Sun, 2015). The angle was measured from 0° to 180° with a measurement accuracy of ± 0.3°. The drop image was recorded by the CCD camera.

2.3.6. Moisture adsorption isotherm

Dynamic vapor sorption (DVS) apparatus (Surface Measurement Systems, London, UK) was used to obtain the moisture adsorption curve of aerogel samples at 25 ℃. A weight change (dm/dt) of less than 0.002%/min over 10 min was chosen as the criterion for reaching equilibrium at each relative humidity (RH) step and then increasing to the next rise or descending RH.

2.3.7. Dry density and porosity estimation

The obtained aerogel weight (m) was determined by an analytical balance (ME204, METTLER TOLEDO, China), and the volume (v) was calculated by its size determined by a vernier caliper. The density (ρ) of the aerogel is calculated by the following formula (Eq. (2)):

$$\rho = \frac{m}{v} \quad (2)$$

Aerogel porosity was estimated based on the method in previous research (Kim, Park, Kim, Wada, & Kaplan, 2005) with minor modification. The aerogel sample was first immersed in ethanol of known volume V1 for 5 min. The volume of the aerogel impregnated with ethanol and ethanol was recorded as V2, and the aerogel impregnated with ethanol was removed. The volume of ethanol is V3, and the porosity (ε) is obtained by the following formula (Eq. (3)):

$$\varepsilon\ (\%) = \frac{(V1-V3)}{(V2-V3)} \times 100\% \quad (3)$$

All experimental data points were analyzed and drawn figures using Origin 2017 (Originlab Corporation, Northanpton MA) and Microsoft Excel 2010. One-way analysis of variance (ANOVA) was performed using statistical product and service solutions (SPSS) (21th edition, Endicott, NY, USA) and the significance of each average property value was determined by measuring Tukey's multi-range test ($p < 0.05$).

3. Results and discussion

3.1. Impact of gelatin on the structure, filtration and mechanical properties of KGM/gelatin aerogel

The formation of ice crystals in the sol led to concentration and aggregation of the solute molecules, and aerogel sample shape was maintained by the aggregated solute molecules during ice crystal sublimation in the lyophilization process, forming a porous network structure (Gutiérrez, Ferrer, & del Monte, 2008). Different network structures might be formed with different solute. As shown in Fig. 1(A1), the SEM image indicted pure KGM aerogel (K1) had a porous three-dimensional network structure, consistent with the previous report (Ni et al., 2016). To demonstrate the impact of gelatin on the change of the pore structure of KGM-gelatin aerogel, SEM images and size distribution (0-240 μm) curves of pores were drawn (Fig. 1(A, B)). Compared with K1, gelatin addition of 1% (K1G1), 2% (K1G2) could bring more micropores and increase pore numbers with pore sizes 0-80 μm by 316.19%, 387.044%, respectively. Therefore, the higher the concentration of gelatin, the higher the number of aerogel pores (0-80 μm) in the range of 0-2%. Gelatin gels changed from disordered single-stranded structure to ordered structure during the formation process with the intrachain hydrogen bonds and interchain hydrogen bonds as the main force, however, the presence of KGM disordered the gelatin coil-helix transition, and this might cause the system to be loose, leading to more pores in the KGM/gelatin aerogel (Khomutov, Lashek, Ptitchkina, & Morris, 1995; Kuijpers, 1999; Jin, Xu, Ge, Li, & Li, 2015).

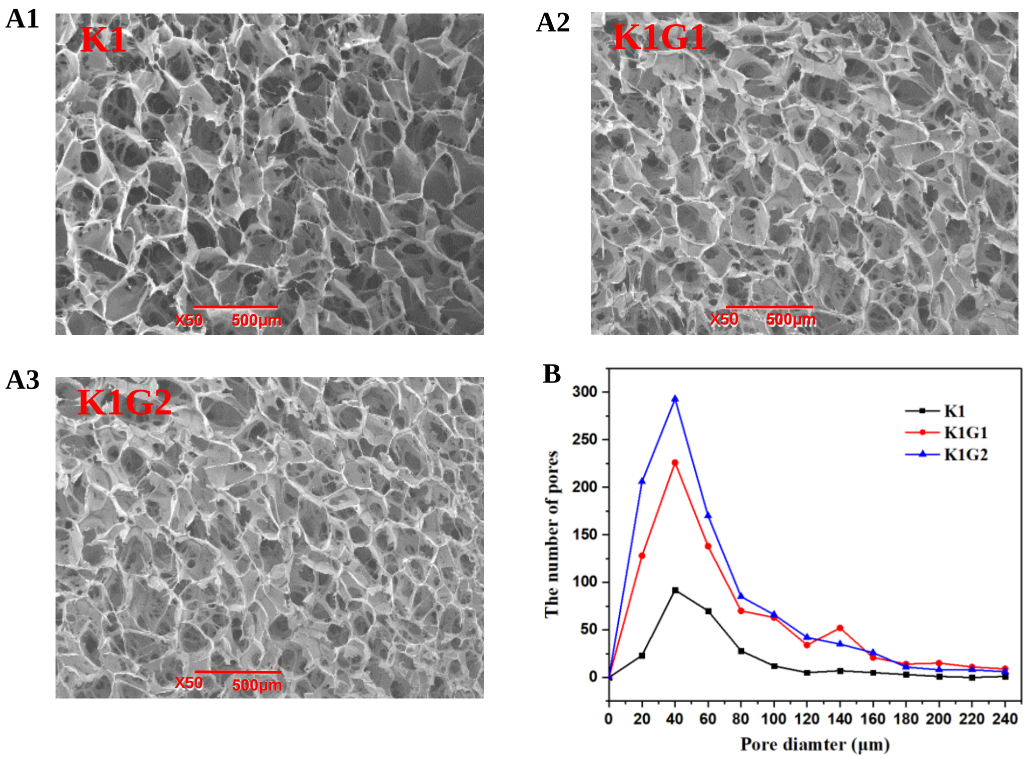

Fig. 2. (A1-A3) SEM images of KGM/gelatin aerogels under magnification 50×; Size distribution (0-240 μm) of KGM/gelatin aerogels pores with different gelatin concentration.

The effect of gelatin addition on KGM/gelatin aerogel filtration efficiency is shown in Fig. 3A. With increased addition of gelatin (1%-2%) (w/v), the filtration efficiency of KGM/gelatin aerogel gradually increased. When further gelatin addition increased to 2%, the filtration efficiency of K1G2 aerogel increased to 57.511% (particle size ≥ 0.3 μm). Fig. 3B showed the filtration resistance of KGM/gelatin aerogel. The filtration resistance of K1 aerogel without gelatin was 7.015 Pa, and with the addition of gelatin, the filtration resistance gradually increased, e.g. the filtration resistance of aerogel with 2% gelatin increased to 59 Pa (Fig. 3B). This was due to the fact that the addition of gelatin could increase the number of small holes (0-80 μm) on the pore wall of KGM/gelatin aerogel (Fig. 2), which might increase the probability of internal inertial collision and Brownian motion of particles (Hutten, 2007), improving the filtration efficiency (Wang & Shen, 2004) and filtration resistance. Improvement in mechanical property is very important for filter materials (Calis Acikbas et al., 2017), and the stress-strain curve (strain 0-30%) of KGM/gelatin aerogel is shown in Fig. 3C. When the addition amount of gelatin was increased from 0% to 1%, the compressive strength was significantly increased, and then it increased slowly with further gelatin addition from 1% to 2% (w/v). The stress of gelatin-added aerogels increased significantly, e.g. from 0.6142 kPa (K1) to 40.5777 kPa (K1G1) and 58.5590 kPa (K1G2). This might be explained by that gelatin and KGM formed an interpenetrating network, and the gel network was enhanced via covalent cross-linking between the complexes (Suo et al., 2018; Liu, Li, Zhang, Li, & Hou, 2018). Therefore, the addition of gelatin not only improved the filtration efficiency of KGM-based aerogel but also increased the compressive stress, facilitating the practical application of KGM-based aerogel as a filter material.

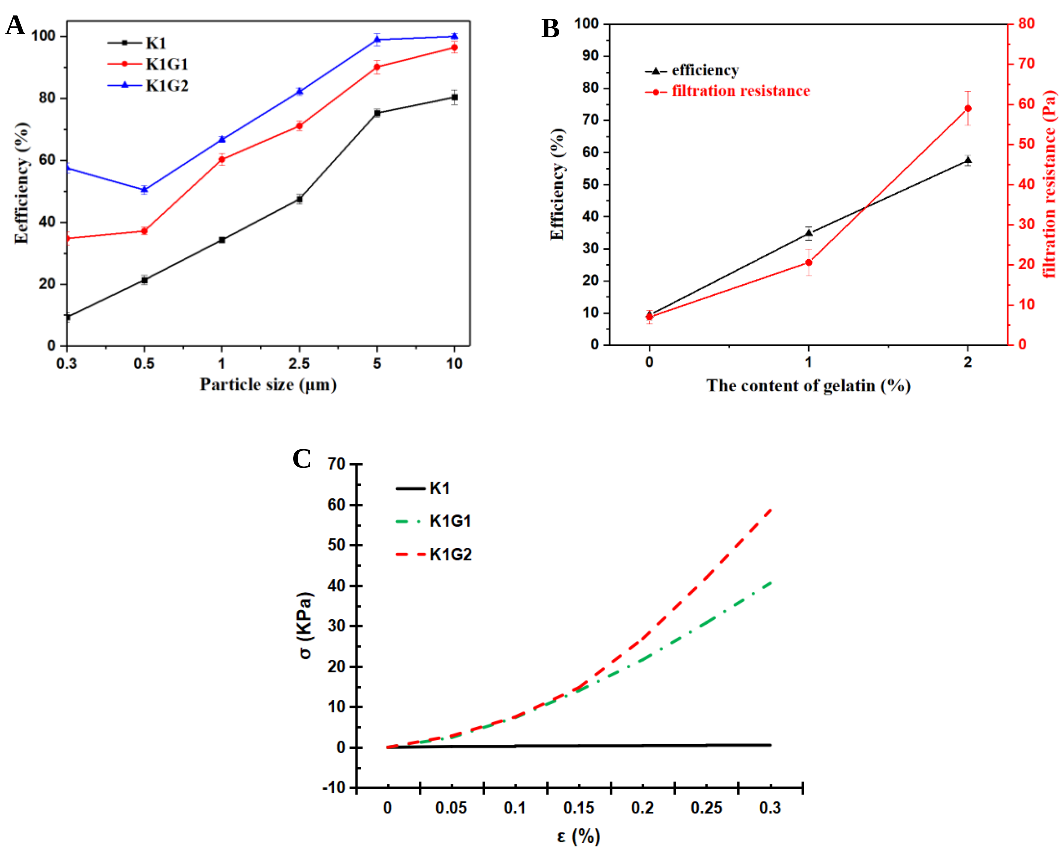

Fig. 3. (A) Filtration efficiency of aerogels with different gelatin concentration for various particle sizes; (B) Filtration efficiency and filtration resistance of aerogels (K1Gn, n=0, 1, 2) for particle matters of 0.3 μm and beyond; (C) Stress-strain curves for KGM/gelatin aerogels with

different gelatin concentration.

3.2. Impact of starch on the structure, filtration property of KGM/starch aerogel

SEM images of KGM/starch aerogels with different starch concentration are shown in Fig. 4. All aerogel samples exhibited a complete, uniform three-dimensional network structure. With increased starch concentration (1%-4%), the pores became smaller, and pores on the pore wall became fewer. The pores were the smallest and the structure was densest when starch concentration was 4%. This could be interpreted as the starch concentration increased, the molecular distance of the system became smaller, reducing spaces for ice crystal growth, and therefore aerogel structure became denser with smaller pores (Qian, Chang, & Ma, 2011).

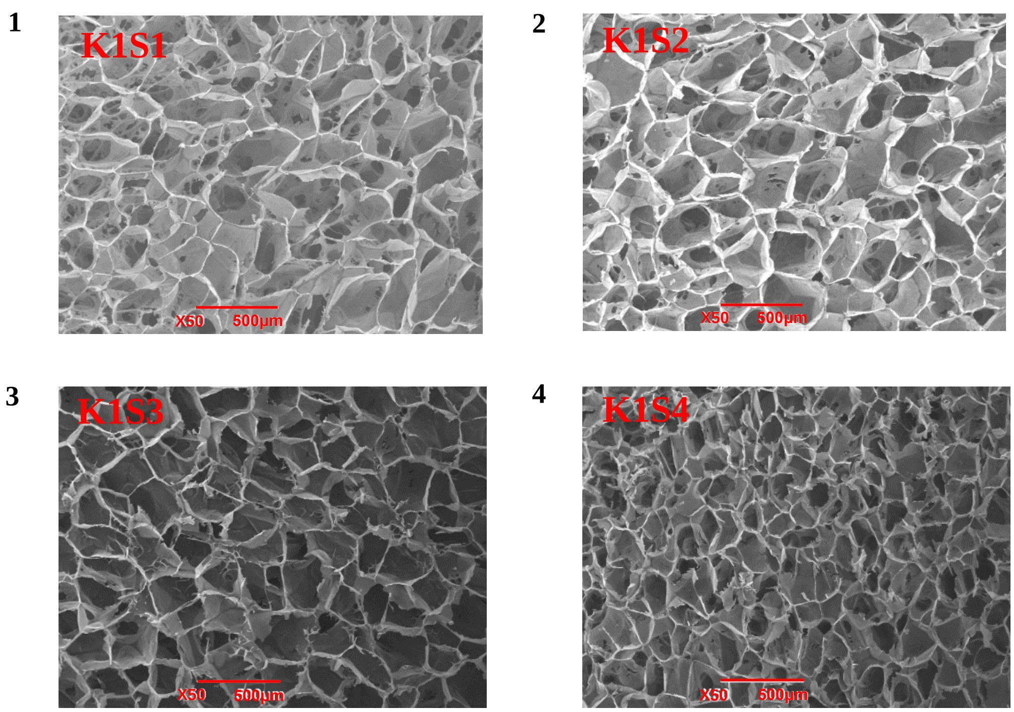

Fig. 4. (1-4) SEM images of KGM/starch aerogel under magnification 50×.

The effect of starch on the filtration efficiency and filtration resistance of KGM/starch aerogel is shown in Fig. 5(A-B). The filtration efficiency of KGM/starch aerogel (starch concentration: 1%-4%

(w/v)) was gradually increased (Fig. 2(A1)), and the filtration efficiency was maximized when starch addition reached 4% (92.78%), but the filtration resistance was overload (>1000 Pa). Based on previous research, the addition of starch could increase the pores with pore sizes range 10-50 μm (Wang et al., 2018), and this might cause an increase in the probability of particles colliding in the aerogel, consuming the kinetic energy of the particles to achieve interception (Lifshutz, & Pierce, 1997). Considering the high resistance is not conducive to the practical application of air filtration material (Wang, Yu, Lai, & Chung, 2018), starch addition was ≤ 3% in the following experiment.

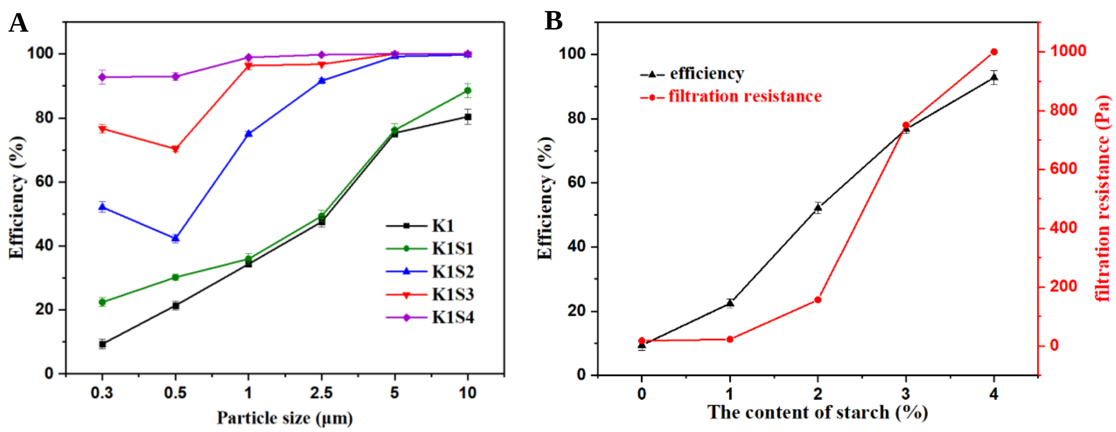

Fig. 5. (A) Filtration efficiency of KGM/starch aerogels with different starch concentration for various particle sizes; (B) Filtration efficiency and filtration resistance of aerogels (K1Sn, n=0, 1, 2, 3, 4) for particle matters of 0.3 μm and beyond.

3.3. Filtration property of KGM/starch/gelatin aerogel

To optimize the component ratio of KGM/gelatin/starch aerogel based on the filtration efficiency, an $L_9(3^3)$ orthogonal array was tested and an optimized aerogel formulation was obtained (Table 1). The highest filtration efficiency was 94.41% (K1G1S3), and the lowest filtration efficiency was 20.40% (K1S1). According to the filtration efficiency, k and range values were calculated, and the results showed the following sequence: starch > gelatin > KGM. The optimized aerogel formula was

K1G1S3 and was used in the following experiments. Its filtration efficiency was 94.41%, and the compression stress was 241.698 kPa.

Table 1

Analysis of $L_9(3)^3$ test results about filtration efficiency.

Sampel code	KGM	Gelatin	Starch	Filtration Efficiency
	(g/100mL)			(Mean ± SD) (%)
K0.5G2S1	0.5	2	1	62.74 ± 1.6015
K0.5G1S2	0.5	1	2	76.47 ± 0.5950
K0.5S3	0.5	0	3	88.63 ± 0.7204
K1S1	1	0	1	22.40 ± 1.4300
K1G2S2	1	2	2	81.35 ± 0.4800
K1G1S3	1	1	3	94.41 ± 0.3953
K1.5G1S1	1.5	1	1	68.73 ± 0.8265
K1.5S2	1.5	0	2	73.89 ± 0.3955
K1.5G2S3	1.5	2	3	82.04 ± 0.3869
k1	75.95	75.38	51.29	
k2	66.05	79.87	77.24	
k3	74.89	61.64	88.36	
range	9.9	18.23	37.07	
Optimal level		S > G > K		
Major factor (w/v)	1%	3%	1%	
Optimized formula		**K1G1S3**		**94.41 ± 0.3953**

3.4. Impact of wheat straw on the structure and filtration property of KGM/gelatin/starch aerogel

Wheat straw in aerogel (K1G1S3WS3) had multi-cavities structure and the pore structure was irregular in SEM images (Fig. 6(A1-A2)). The filtration property of KGM/gelatin/starch/wheat straw aerogel is shown in Fig. 6B. As wheat straw concentration increased from 0% to 0.5% (w/v), the filtration efficiency was reduced from 94.41% to 62.59% (particle matters ≥ 0.3 μm), and the filtration resistance was reduced from 921 Pa to 117.67 Pa. The filtration efficiency of aerogel (K1G1S3WS2.5) was increased to a maximum value of 93.54% (particle matters ≥ 0.3 μm). The filtration resistance was continued to decrease until below 50 Pa when wheat straw concentration ≥0.5% (w/v). Air permeability is also an important indicator of filter materials, affecting the filtration efficiency of filter materials (Woudberg, Theron, Lys, & Le Coq, 2018). The air permeability of aerogel with wheat straw addition is shown in Fig. 6C. With increased addition of wheat straw (0%-1.5% (w/v)), the air permeability started to increase significantly (27.33-257.02 L/s·m^2), and then it became to change slightly when the wheat straw addition was further increased from 2% to 3% (w/v). The highest air permeability (271.42 L/s·m^2) of aerogel (K1G1S3WS3) was reached with 3% wheat straw addition, and the density and porosity were 0.1050 ± 0.0008 g/cm^3 and 92.13 ± 0.04%, respectively. Similar to wood cells, wheat straw is also a porous material with the micro cellular structure (Strømdahl, 2000), thus the pore structure of K1G1S3 aerogel might be affected due to cavity structure of wheat straw, resulting in a decrease in the filtration efficiency of the aerogel. However, the micro cellular structure also increased microchannel inside aerogel, so the filtration efficiency (Liu et al., 2019) and air permeability (Wang, Cai, Yang, & Yang, 2018) increased with increased wheat straw concentration.

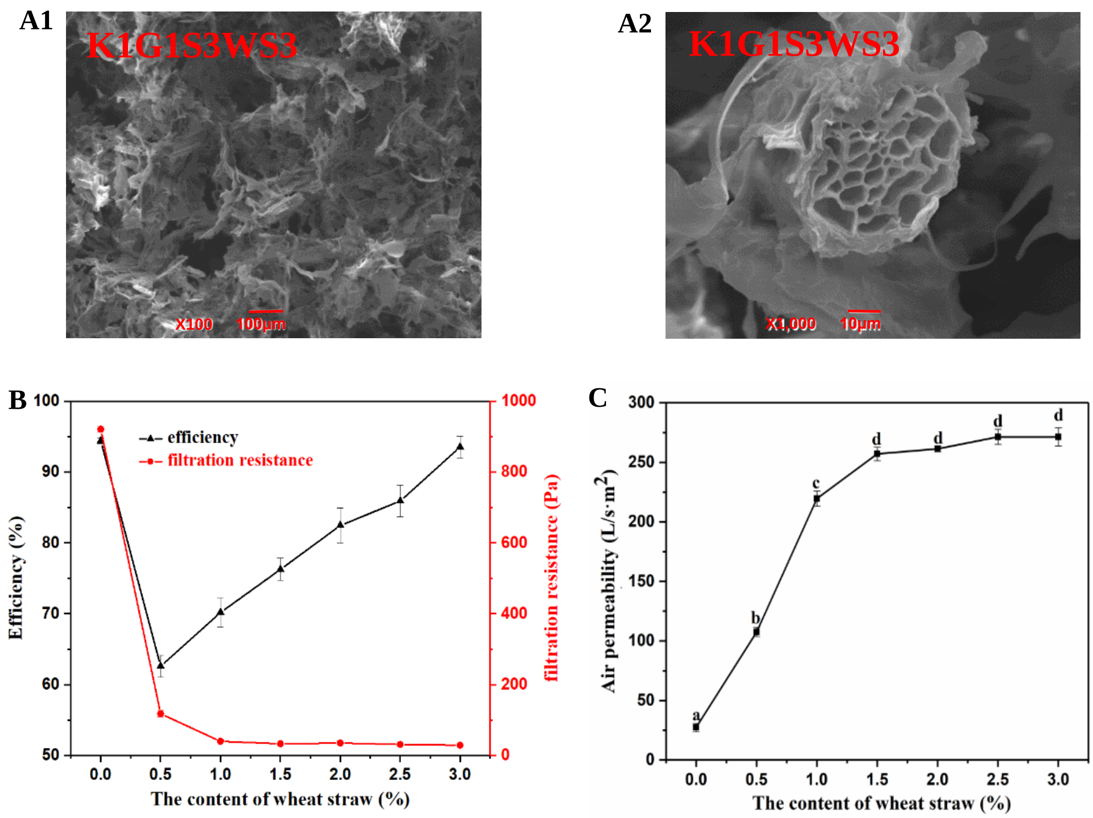

Fig. 6. (A) SEM images of K1G1S3WS3 under magnification 100× (A1), 1000× (A2). (B) Filtration efficiency and filtration resistance of aerogels (K1G1S3WSn, n=0, 0.5, 1, 1.5, 2, 2.5, 3) for particle matters of 0.3 μm and beyond; (C) Air permeability of aerogels (K1G1S3WSn, n=0, 0.5, 1, 1.5, 2, 2.5, 3), data points with the different letter are significantly different.

3.5. Impact of okara on the structure and hydrophobic property of KGM/gelatin/starch aerogel

The impact of okara addition on the hydrophobicity improvement of aerogel was studied based on K1G1S3 aerogel sample. The pore shape of K1G1S3O2 aerogel was more disordered than K1 (Fig. 2(A1)), and a special structure of agglomeration occurred in Fig. 7(A2), by the fact that the special lumpy structure of insoluble dietary fiber in okara (Mateos-Aparicio, Mateos-Peinado, & Rupérez, 2010) was uniformly dispersed in the aerogel and caused shape changes of the pore structure of the aerogel (Kiani & Sun, 2011). The analysis of the FTIR spectra is shown in Fig. 7B. The stretching bands of 2923.59, 2924.48, 2921.36, 2925.63, 2883.23, 2892.84, 2882.52, and 2888.12 cm^{-1} were assigned to C-H. Comparing the spectra of K1, K1G1, K1S1, K1G1S3 and K1G1S3On aerogels (n=0.5, 1, 1.5, 2), the addition of okara caused a shift of the C-H stretching bands to the higher frequencies (“blueshift”), which may be caused by hydrophobic interaction of the methyl groups (Schmidt, Dybal, & Trchová, 2006). The insoluble components in the okara might act as a special structure in Fig. 7(A2) in aerogel and the aerogel might be therefore hydrophobic. The density and porosity of K1G1S3O2 were 0.0752 ± 0.0009 g/cm^3 and 90.30 ± 0.05%, respectively.

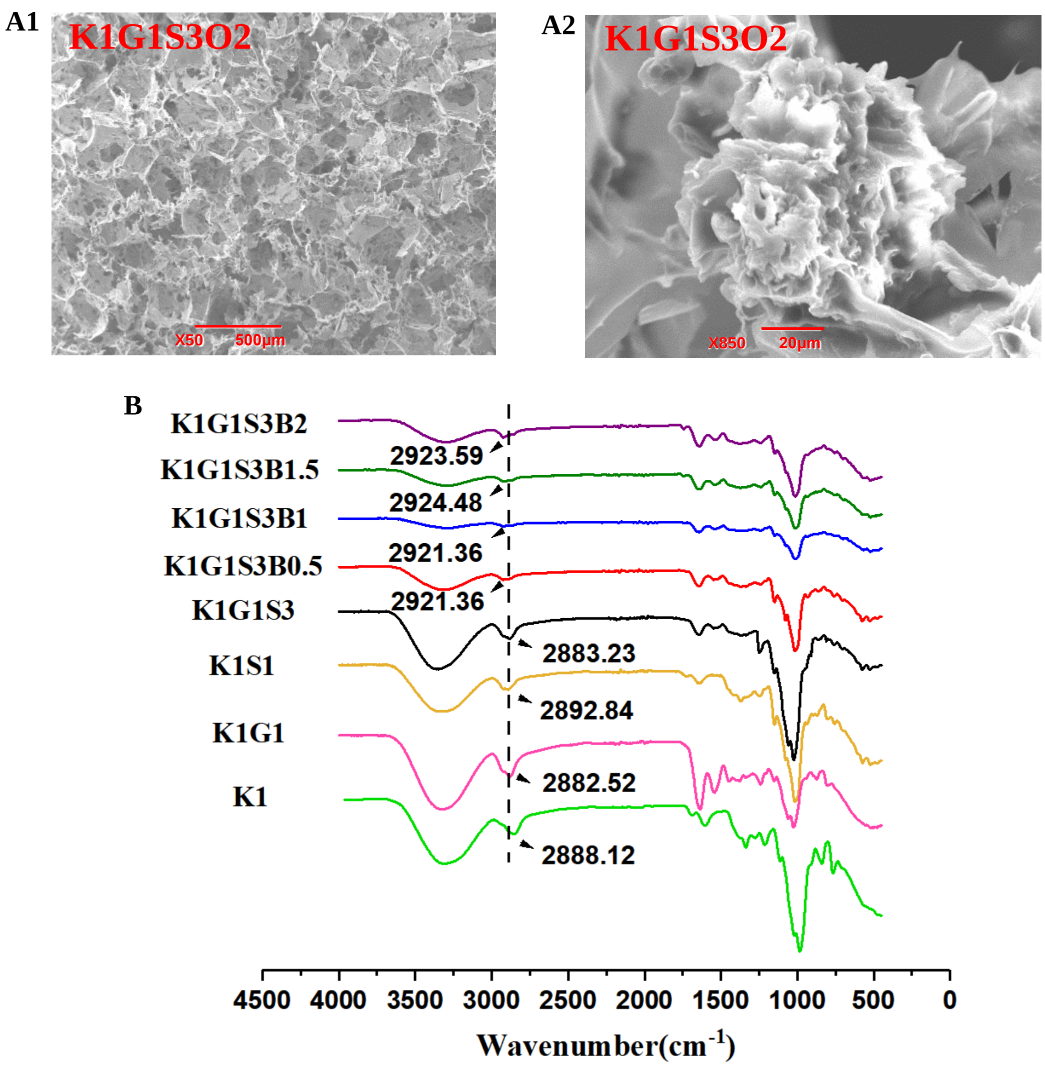

Fig. 7. (A) SEM images of K1G1S3O2 under magnification 50× (A1), 850× (A2); (B) FT-IR spectra of aerogels (K1, K1G1, K1S1, K1G1S3, and K1G1S3On, (n=0.5, 1, 1.5, 2)).

Generally, the greater the water contact angle, the higher the surface hydrophobicity (Yin et al., 2014;

Escamilla-García et al., 2013). The effect of okara addition on the water contact angle of KGM/gelatin/starch aerogel is shown in Fig. 8. The water contact angle of the aerogel without okara addition (K1G(1-2), K1S(1-4), and K1G1S3) was 0°. K1G1S3 aerogel is composed of polysaccharide and proteins with high polar groups, which easily destroyed the cohesion of water molecules and resulted in a low water contact angle (Kaity et al., 2013). With okara concentration increased from 0% to 1.5% (w/v), the water contact angle began to significantly increase. Further increase of the okara concentration (1.5% to 2.0%) resulted in a slight increase of the water contact angle till reaching the maximum value 105.4° (2% (K1G1S3O2)). The material with water contact angle ≥90° is hydrophobic and has good hydrophobicity (Chen, Wang, & Shi, 2017; Wu et al., 2017; Scaffaro, Sutera, & Botta, 2018). The presence of okara containing insoluble protein might increase the amount of non-polar substances on the surface of aerogel, which increased the water contact angle.

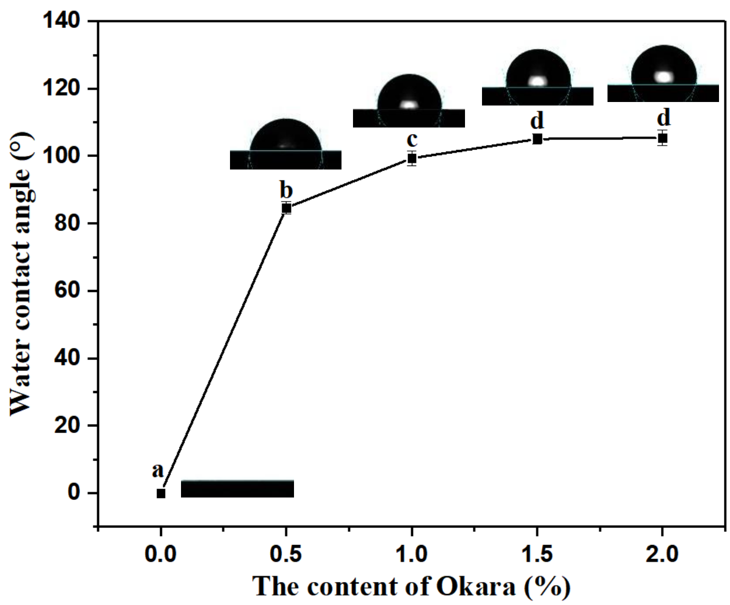

Fig. 8. Water contact angle of aerogels (K1G1S3On, n=0.5, 1, 1.5, 2), data points with the different letter are significantly different.

The moisture adsorption isotherms (Fig. 9) showed Type II-b shape according to Blahovec and Yanniotis's research classification (Blahovec, & Yanniotis, 2009), which was consistent with the moisture adsorption isotherms of most materials (Mohammadi Nafchi, Moradpour, Saeidi, & Alias, 2014; Bingol, Prakash, & Pan, 2012). The experiment results showed that the aerogel with different content of okara all exhibited less equilibrium water concentration compared with K1G1S3 aerogel in the ranges of RH 0%-80%, and the equilibrium water content of K1G1S3O2 was reduced by 17.03%-81.10% compared with K1G1S3. This further demonstrated that hydrophobicity of KGM-based aerogel with okara was improved.

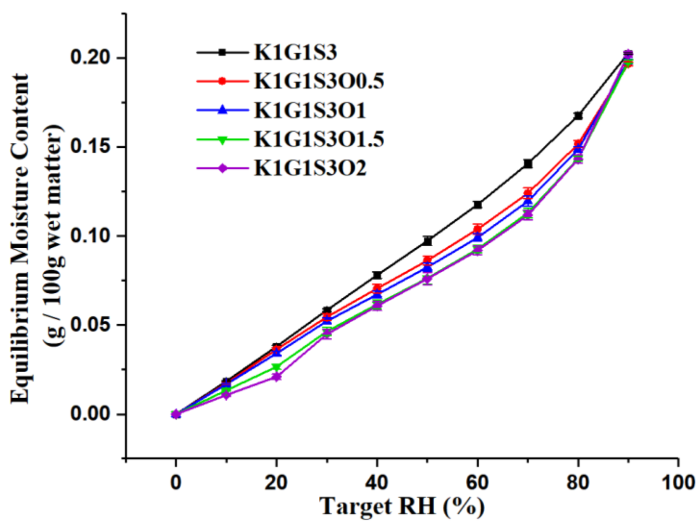

Fig. 9. Water adsorption isotherms of aerogels (K1G1S3On, n=0.5, 1, 1.5, 2) at 25℃ determined by DVS.

4. Conclusions

The KGM-based aerogel with enhanced filtration, mechanical and hydrophobic properties was prepared. Gelatin and starch components caused the appearance of more microporous pore structure and the formation of the dense structure of KGM-based aerogel network, which could improve the mechanical and filtration properties of KGM-based aerogel. The addition of wheat straw could decrease the filtration resistance and increase the breathability of KGM-based aerogel, which was attributed to the multi-cavities of wheat straw. Okara addition could make KGM-based aerogel more hydrophobic by increasing surface water contact angle and decreasing equilibrium water content of aerogel. The data revealed that aerogel containing 3% wheat straw (K1G1S3WS3) has a filtration efficiency 93.54 ± 1.5450% (particle matters (DEHS) ≥ 0.3 μm), a filtration resistance 29 Pa, an air permeability 271.42 L/s·m^2, and a compressive strength 241.698 kPa. The water contact angle of the aerogel containing 2% (w/v) okara (K1G1S3O2) reached the maximum value 105.4°, and the equilibrium water content of K1G1S3O2 was 17.03%-81.10% lower than K1G1S3, with RH 0%-80%. This study enhanced the practicality of KGM-based aerogel as air filtration material.

Acknowledgment

This work was financially supported by the European Commission for the H2020 Marie Skłodowska-Curie Actions Individual Fellowships 2017 Project (Grant ID: 794680) and National Natural Science Foundation of China (Grant ID: 31671827 and 31801582).

References

Anderson, J. O., Thundiyil, J. G., & Stolbach, A. (2011). Clearing the air: a review of the effects of particulate matter air pollution on human health. *Journal of Medical Toxicology*, *8*(2), 166-175.

Antonicelli, L., Bilò, M.B., Pucci, S., Schou, C., & Bonifazi, F. (1991). Efficacy of an air leaning device equipped with a high efficiency particulate air filter in house dust mite respiratory allergy. *Allergy*, *46*(8), 594-600.

Akbarnezhad, S., Amini, A., Goharrizi, A. S., Rainey, T., & Morawska, L. (2017). Capacity of quartz fibers with high filtration efficiency for capturing soot aerosol particles. *International Journal of Environmental Science & Technology*,*15*(5), 1-10.

Brunekreef, B., & Hoffmann, B. (2016). Air pollution and heart disease. *The Lancet, 388*, 640-642.

Blahovec, J., & Yanniotis, S. (2009). Modified classification of sorption isotherms. *Journal of Food Engineering*, *91*, 72-77.

Bingol, G., Prakash, B., & Pan, Z. (2012). Dynamic vapor sorption isotherms of medium grain rice varieties. *LWT - Food Science and Technology, 48*(2), 156-163.

Chow, J. C., Watson, J. G., Mauderly, J. L., Costa, D. L., Wyzga, R. E., Vedal, S., & Dockery, D. W. (2006). Health effects of fine particulate air pollution: lines that connect. *Journal of the Air & Waste*

Management Association, 56(10), 1368-1380.

Cohen, A. J., Ross Anderson, H., Ostro, B., Pandey, K. D., Krzyzanowski, M., Künzli, N., Gutschmidt, K., Pope, A., Romieu, I., Samet, J. M., & Smith, K. (2005). The global burden of disease due to outdoor air pollution. *Journal of Toxicology and Environmental Health, Part A, 68*(13-14), 1301-1307.

Chen, X., Kuang, Y., Xiao, M., Wu, K., Yan, W., Jiang, F., & Huang, J. (2017). Study on adsorption of plant polysaccharide aerogels. *Science and Technology of Food Industry*, *38*(11), 96-101.

Corobea, M. C., Muhulet, O., Miculescu, F., Antoniac, I. V., Vuluga, Z., Florea, D., Vulugad, D. M., Butnarue, M., Ivanovf, D., & Voicu, S. I. (2016). Novel nanocomposite membranes from cellulose acetate and clay- silica nanowires. *Polymers for Advanced Technologies, 27*(12), 1586-1595.

Calis Acikbas, N., Ture, Y., Gurlek, E., Ozcan, S., Soylu, S., Acikbas, G., & Gudu, T. (2017). Microstructural characterization, mechanical, physical and thermal properties of a diesel particulate filter. *Arabian Journal for Science and Engineering, 43*, 1383-1394.

Chen, G., Wang, Z. L., & Shi, Y. (2017). *Preparation method of superhydrophobic film*. [(Pattern NO.;1; 107723687). CN].

Davé, V., & McCarthy, S. P. (1997). Review of Konjac glucomannan. *Journal of Environmental Polymer Degradation*, *5*(4), 237.

Escamilla-García, M., Calderón-Domínguez, G., Chanona-Pérez, J.J., Farrera-Rebollo, R. R., Andraca-Adame, J. A., Arzate-Vázquez, I., Moreno-Ruiz, L. A., & Mendez-Mendez J.V. (2013). Physical and structural characterisation of zein and chitosan edible films using nanotechnology tools. *International Journal of Biological Macromolecules, 61*, 196-203.

Fang, W., & Wu, P. (2004). Variations of konjac glucomannan (KGM) from Amorphophallus konjac and its refined powder in China. *Food Hydrocolloids, 18*(1), 167-170.

Gurjar, B. R., Jain, A., Sharma, A., Agarwal, A., Gupta, P., Nagpure, A. S., & Lelieveld, J. (2010). Human health risks in megacities due to air pollution. *Atmospheric Environment, 44*(36), 4606-4613.

García-González, C. A., Uy, J. J., Alnaief, M., & Smirnova, I. (2012). Preparation of tailor-made starch-based aerogel microspheres by the emulsion-gelation method. *Carbohydrate Polymers, 88*(4), 1378-1386.

Gutiérrez, M. C., Ferrer, M. L., & del Monte, F. (2008). Ice-templated materials: sophisticated structures exhibiting enhanced functionalities obtained after unidirectional freezing and ice-segregation-induced self-assembly. *Chemistry of Materials, 20*(3), 634-648.

Huang, G., Li, F., Zhao, X., Ma, Y., Li, Y., Lin, M., Jin, G., Lu, T., Genin, G. M., & Xu, F. (2017). Functional and biomimetic materials for engineering of the three-dimensional cell. *Chemical Reviews, 117*(20), 12764-12850.

Hutten, I. M. (2007). Hutten I M. Handbook of nonwoven filter media. *AATCC Review, 7*(9), 8-8.

Jiamjariyatam, R., Kongpensook, V., & Pradipasena, P. (2014). Effects of amylose content, cooling rate and aging time on properties and characteristics of rice starch gels and puffed products. *Journal of Cereal Science, 61*, 16-25.

Jin, C., Han, S., Li, J., & Sun, Q. (2015). Fabrication of cellulose-based aerogels from waste newspaper without any pretreatment and their use for absorbents. *Carbohydrate Polymers, 123*, 150-156.

Jin, W., Xu, W., Ge, H., Li, J., & Li, B. (2015). Coupling process of phase separation and gelation in konjac glucomannan and gelatin system. *Food Hydrocolloids, 51*, 188-192.

Kim, S. J., Chase, G., & Jana, S. C. (2015). Polymer aerogels for efficient removal of airborne nanoparticles. *Separation & Purification Technology, 156*, 803-808.

Kang, H. W., Tabata, Y., & Ikada, Y. (1999). Fabrication of porous gelatin scaffolds for tissue engineering. *Biomaterials, 20*(14), 1339-1344.

Kim, U. J., Park, J., Kim, H. J., Wada, M., & Kaplan, D. L. (2005). Three-dimensional aqueous-derived biomaterial scaffolds from silk fibroin. *Biomaterials, 26*(15), 2775-2785.

Kaity, S., Isaac, J., Kumar, P. M., Bose, A., Wong, T. W., & Ghosh, A. (2013). Microwave assisted synthesis of acrylamide grafted locust bean gum and its application in drug delivery. *Carbohydrate Polymers, 98*(1), 1083-1094.

Khomutov, L. I., Lashek, N. A., Ptitchkina, N. M., & Morris, E. R. (1995). Temperature-composition phase diagram and gel properties of the gelatin-starch-water system. *Carbohydrate Polymers, 28*(4), 341-345.

Kuijpers, A. J., Engbers, G. H. M., Feijen, J., De Smedt, S. C., Meyvis, T. K. L., Demeester, J., Krijgsveld, J., Zaat, S. A. J., & Dankert, J. (1999). Characterization of the network structure of carbodiimide cross-Linked gelatin gels. *Macromolecules, 32*(10), 3325-3333.

Kiani, H., & Sun, D. W. (2011). Water crystallization and its importance to freezing of foods: a review. *Trends in Food Science & Technology, 22*(8), 407-426.

Landrigan, P. J. (2017). Air pollution and health. *The Lancet Public Health, 2*(1), e4-e5.

Li, B., Zhou, F., Huang, K., Wang, Y., Mei, S., Zhou, Y., & Jing, T. (2016). Highly efficient removal of lead and cadmium during wastewater irrigation using a polyethylenimine-grafted gelatin sponge. *Scientific Reports, 6*(1), 33573.

Liu, Y., Li, B., Zhang, K., Li, J., & Hou, H. (2018). Novel hard capsule prepared by tilapia (Oreochromis niloticus) scale gelatin and konjac glucomannan: characterization, and in vitro dissolution. *Carbohydrate Polymers, 206*, 254-261.

Lifshutz, N., & Pierce, M. (1997). A general correlation of mpps penetration as a function of face velocity with the model 8140 using the certitest 8160. *Acta Palaeontologica Polonica,46*(3), 367-376.

Liu, J., Ren, B., Wang, Y., Lu, Y., Wang, L., Chen, Y., Yang, J., & Huang, Y. (2019). Hierarchical porous ceramics with 3D reticular architecture and efficient flow-through filtration towards high-temperature particulate matter capture. *Chemical Engineering Journal, 362*, 504-512.

Mateos-Aparicio, I., Redondo-Cuenca, A., Villanueva-Suárez, M. J., Zapata-Revilla, M. A., & Tenorio-Sanz, M. D. (2010). Pea pod, broad bean pod and okara, potential sources of functional compounds. *LWT-Food Science and Technology, 43*(9), 1467-1470.

Mateos-Aparicio, I., Mateos-Peinado, C., & Rupérez, P. (2010). High hydrostatic pressure improves the functionality of dietary fibre in okara by-product from soybean. *Innovative Food Science & Emerging Technologies, 11*(3), 445-450.

Mohammadi Nafchi, A., Moradpour, M., Saeidi, M., & Alias, A. K. (2014). Effects of nanorod-rich zno on rheological, sorption isotherm, and physicochemical properties of bovine gelatin films. *LWT-Food Science and Technology, 58*(1), 142-149.

Ni, X., Ke, F., Xiao, M., Wu, K., Kuang, Y., Corke, H., & Jiang, F. (2016). The control of ice crystal growth and effect on porous structure of konjac glucomannan-based aerogels. *International Journal of Biological Macromolecules, 92,* 1130-1135.

Pope III, C. A. (2002). Lung cancer, cardiopulmonary mortality, and long-term exposure to fine particulate air pollution. *JAMA, 287*(9), 1132-1141.

Park, J. H., Yoon, K. Y., & Hwang, J. (2011). Removal of submicron particles using a carbon fiber ionizer-assisted medium air filter in a heating, ventilation, and air-conditioning (HVAC) system. *Building and Environment*, *46*(8), 1699-1708.

Pigeot-Remy, S., Lazzaroni, J. C., Simonet, F., Petinga, P., Vallet, C., Petit, P., Vallet, C., Petit, P., Vialle, P. J., & Guillard, C. (2014). Survival of bioaerosols in HVAC system photocatalytic filters. *Applied Catalysis B: Environmental, 144,* 654-664.

Qian, D., Chang, P. R., & Ma, X. (2011). Preparation of controllable porous starch with different starch concentrations by the single or dual freezing process. *Carbohydrate Polymers,86*(3), 1181-1186.

Russell, A. G., & Brunekreef, B. (2009). A focus on particulate matter and health. *Environmental Science & Technology*, *43*(13), 4620-4625.

Redondo-Cuenca, A., Villanueva-Suárez, M. J., & Mateos-Aparicio, I. (2008). Soybean seeds and its by-product okara as sources of dietary fibre. Measurement by AOAC and Englyst methods. *Food Chemistry, 108*(3), 1099-1105.

Sutherland, K. (2008). Air filtration: using filtration to control industrial air pollution. *Filtration & Separation*, *45*(9), 16-19.

Suarez, S., Hewer, T. L. R., Portela, R., Hernandezalonso, M. D., Freire, R. S., & Sanchez, B. (2011). Behaviour of tio 2-simgo x hybrid composites on the solar photocatalytic degradation of polluted air. *Applied Catalysis B Environmental*, *101*(3-4), 176-182.

Shi, J., Lu, L., Guo, W., Liu, M., & Cao, Y. (2015). On preparation, structure and performance of high porosity bulk cellulose aerogel. *Plastics, Rubber and Composites, 44*(1), 26-32.

Suo, H., Zhang, D., Yin, J., Qian, J., Wu, Z., & Fu, J. (2018). Interpenetrating polymer network hydrogels composed of chitosan and photocrosslinkable gelatin with enhanced mechanical properties for tissue engineering. *Materials Science and Engineering: C, 92*, 612-620.

Strømdahl, K. (2000). Water Sorption in Wood and Plant Fibres. Technical University of Denmark, Danmarks Tekniske Universitet, Department of Structural Engineering and Materials Institut for Bærende Konstruktioner og Materialer.

Schmidt, P., Dybal, J., & Trchová, M. (2006). Investigations of the hydrophobic and hydrophilic interactions in polymer-water systems by ATR FTIR and Raman spectroscopy. *Vibrational Spectroscopy, 42*(2), 278-283.

Scaffaro, R., Sutera, F., & Botta, L. (2018). Biopolymeric bilayer films produced by co-extrusion film blowing. *Polymer Testing*, *65*, 35-43.

Tang, M., Chen, S. C., Chang, D., Xie, X., Sun, J., & Pui, D. Y. H. (2018). Filtration efficiency and loading characteristics of $PM_{2.5}$ through composite filter media consisting of commercial HVAC electret media and nanofiber layer. *Separation and Purification Technology, 198*, 137-145.

Wang, Z., Huang, Y., Wang, M., Wu, G., Geng, T., Zhao, Y., & Wu, A. (2016). Macroporous calcium alginate aerogel as sorbent for Pb^{2+} removal from water media. *Journal of Environmental Chemical Engineering, 4*(3), 3185-3192.

Wang, Y., Chen, X., Kuang, Y., Jiang, F., & Yan, W. (2017). Progress in application of polysaccharide aerogels. *Journal of Wuhan Institue of Technology, 39*(5), 443-449.

Wang, Y., Wu, K., Xiao, M., Riffat, S. B., Su, Y., & Jiang, F. (2018). Thermal conductivity, structure and mechanical properties of konjac glucomannan/starch based aerogel strengthened by wheat straw. *Carbohydrate Polymers, 197*, 284-291.

Wang, J., Zhao, D., Shang, K., Wang, Y., Ye, D., Kang, A., Liao, W., & Wang, Y. (2016). Ultrasoft gelatin aerogels for oil contaminant removal. *Journal of Materials Chemistry A, 4*(24), 9381-9389.

Wang, Y., Zhao, H., Degracia, K., Han, L., Sun, H., Sun, M., Wang, Y., & Schiraldi, D. A. (2017). Green approach to improving the strength and flame retardancy of poly (vinyl alcohol)/clay aerogels: incorporating biobased gelatin. *ACS Applied Materials & Interfaces, 9*, 42258-42265.

Wang, D., & Shen, Z. (2004). Pore structure characteristics of deposits formed during fiber bundle media filtration. *Particuology, 2*(3), 128-131.

Wang, L. Y., Yu, L. E., Lai, J. Y., & Chung, T. S. (2018). Developing ultra-high gas permeance PVDF hollow fibers for air filtration applications. *Separation and Purification Technology, 205*, 184-195.

Woudberg, S., Theron, F., Lys, E., & Le Coq, L. (2018). Investigating the influence of local porosity variations and anisotropy effects on the permeability of fibrous media for air filtration. *Chemical Engineering Science*, *180*, 70-78.

Wang, N., Cai, M., Yang, X., & Yang, Y. (2018). Electret nanofibrous membrane with enhanced filtration performance and wearing comfortability for face mask. *Journal of Colloid and Interface Science*, *530*, 695-703.

Wu, K., Zhu, Q., Qian, H., Xiao, M., Corke, H., Nishinari, K., & Jiang, F. (2018). Controllable hydrophilicity-hydrophobicity and related properties of konjac glucomannan and ethyl cellulose composite films. *Food Hydrocolloids*, *79*, 301-309.

Xu, M., Bao, W., Xu, S., Wang, X., & Sun, R. (2015). Porous cellulose aerogels with high mechanical performance and their absorption behaviors. *BioResources*, *11*(1), 8-20.

Yin, Y., Yin, S., Yang, X., Tang, C., Wen, S., Chen, Z., Xiao, B., & Wu, L. (2014). Surface modification of sodium caseinate films by zein coatings. *Food Hydrocolloids*, *36*(2), 1-8.

Zhu, J., Hu, J., Jiang, C., Liu, S., & Li, Y. (2018). Ultralight, hydrophobic, monolithic konjac glucomannan-silica composite aerogel with thermal insulation and mechanical properties. *Carbohydrate Polymers*, *207*, 246-255.